Neuronal injury and tumor necrosis factor-alpha immunoreactivity in the rat hippocampus in the early period of asphyxia-induced cardiac arrest under normothermia

Hyun-Jin Tae[1, #], Il Jun Kang[2, #], Tae-Kyeong Lee[3], Jeong Hwi Cho[3], Jae-Chul Lee[3], Myoung Cheol Shin[4], Yoon Sung Kim[4, 5], Jun Hwi Cho[4], Jong-Dai Kim[6], Ji Hyeon Ahn[7], Joon Ha Park[7], In-Shik Kim[1], Hyang-Ah Lee[8], Yang Hee Kim[9], Moo-Ho Won[3, *], Young Joo Lee[10, *]

1 Bio-Safety Research Institute, College of Veterinary Medicine, Chonbuk National University, Iksan, South Korea
2 Department of Food Science and Nutrition, Hallym University, Chuncheon, South Korea
3 Department of Neurobiology, School of Medicine, Kangwon National University, Chuncheon, South Korea
4 Department of Emergency Medicine, School of Medicine, Kangwon National University, Chuncheon, South Korea
5 Department of Emergency Medicine, Samcheok Medical Center, Samcheok, South Korea
6 Division of Food Biotechnology, School of Biotechnology, Kangwon National University, Chuncheon, South Korea
7 Department of Biomedical Science, Research Institute of Bioscience and Biotechnology, Hallym University, Chuncheon, South Korea
8 Department of Obstetrics and Gynecology, School of Medicine, Kangwon National University, Chuncheon, South Korea
9 Department of Surgery, School of Medicine, Kangwon National University, Chuncheon, South Korea
10 Department of Emergency Medicine, Seoul Hospital, College of Medicine, Sooncheonhyang University, Seoul, South Korea

Abstract

Low survival rate occurs in patients who initially experience a spontaneous return of circulation after cardiac arrest (CA). In this study, we induced asphyxial CA in adult male Sprague-Daley rats, maintained their body temperature at 37 ± 0.5°C, and then observed the survival rate during the post-resuscitation phase. We examined neuronal damage in the hippocampus using cresyl violet (CV) and Fluore-Jade B (F-J B) staining, and pro-inflammatory response using ionized calcium-binding adapter molecule 1 (Iba-1), glial fibrillary acidic protein (GFAP), and tumor necrosis factor-alpha (TNF-α) immunohistochemistry in the hippocampus after asphyxial CA in rats under normothermia. Our results show that the survival rate decreased gradually post-CA (about 63% at 6 hours, 37% at 1 day, and 8% at 2 days post-CA). Rats were sacrificed at these points in time post-CA, and no neuronal damage was found in the hippocampus until 1 day post-CA. However, some neurons in the stratum pyramidale of the CA region in the hippocampus were dead 2 days post-CA. Iba-1 immunoreactive microglia in the CA1 region did not change until 1 day post-CA, and they were activated (enlarged cell bodies with short and thicken processes) in all layers 2 days post-CA. Meanwhile, GFAP-immunoreactive astrocytes did not change significantly until 2 days post-CA. TNF-α immunoreactivity decreased significantly in neurons of the stratum pyramidale in the CA1 region 6 hours post-CA, decreased gradually until 1 day post-CA, and increased significantly again 2 days post-CA. These findings suggest that low survival rate of normothermic rats in the early period of asphyxia-induced CA is related to increased TNF-α immunoreactivity, but not to neuronal damage in the hippocampal CA1 region.

Key Words: nerve regeneration; post-cardiac arrest syndrome; normothermia; neuronal damage; gliosis; tumor necrosis factor-alpha; neural regeneration

Introduction

Cardiac arrest (CA) refers to the abrupt stop in blood flow to the body due to a failure of the heart to continue pumping blood (Girotra et al., 2015). Morbidity and mortality is high in patients who achieve a return of spontaneous circulation (RoSC) after CA due to post-cardiac arrest syndrome (PCAS) (Girotra et al., 2015; Laubach and Sharma, 2016). Many studies on CA have focused on improving the rate of RoSC with significant progress. However, the survival rate is low with a poor prognosis (Neumar et al., 2008; Mongardon et al., 2011; Lopez-Herce et al., 2014).

The low survival rate following CA is ascribed to a unique pathophysiological process_ENREF_1 called PCAS (Girotra et al., 2015). PCAS involves all clinical and biological manifestations including myocardial dysfunction and central nervous system injury, showing a persistent precipitating pathology (Lopez-Herce et al., 2014). Roberts et al. (2013) have reported that dysfunctions are common in multiple organs after RoSC

following CA, and they suggest that multi-organ dysfunction is associated with a low survival rate.

The pathophysiological process of PCAS results in ischemia/reperfusion (IR)-mediated damage in the whole-body, showing non-specific activation of a systemic inflammatory response, triggered by CA and RoSC _ENREF_2 (Mongardon et al., 2011). In general, an inflammatory response occurs due to an infection. However, 'sterile inflammation' occurs in cases with ischemic insults (Laubach and Sharma, 2016). IR injury after CA leads to the release of inflammatory cytokines, which evokes a systemic inflammatory response syndrome, even with no infection (Bro-Jeppesen et al., 2015).

There is no doubt that brain damage is critical in PCAS, and many studies have focused on brain injury and dysfunction after RoSC following CA (Laurent et al., 2002; Madl and Holzer, 2004). However, the exact relationship between the low survival rate and brain damage in the early stage after RoSC following CA remains unclear until now.

Recently, it has been reported that tumor necrosis factor-alpha (TNF-α) protein levels are increased in the heart and lung of animal models of CA (Qi et al., 2013; Drabek et al., 2014b; Zhao et al., 2015). Moreover, tumor necrosis factor-alpha (TNF-α) is changed in the brain after CA in rats (Drabek et al., 2014b). However, the relationship between TNF-α change in the brain and low survival rate remains unclear in the early stage of RoSC after CA.

Therefore, we hypothesized that IR following CA causes inflammatory response in the brain, which leads to neurological dysfunction and alteration of pro-inflammatory factors. In this regard, the inflammatory response in the brain after CA should be studied in the early stage after CA to identify the relationship of a low survival rate with PCAS. Therefore, in this study, we developed a rat model of asphyxial CA, figured the survival rate after CA, and examined neuronal damage/death in the hippocampus, which is susceptible to transient ischemia, to identify its relationship with a low survival rate in the early stage after CA. In addition, we investigated alterations in TNF-α as a pro-inflammatory cytokine by conducting immunohistochemistry after RoSC.

Materials and Methods

Animals

We used male rats (Sprague-Dawley, 12 weeks, weighing 300–320 g, total $n = 56$), which were raised in the Experimental Animal Center of Kangwon National University (Chuncheon, Republic of Korea). The procedure for animal handling and care adhered to the guidelines that are in compliance with the current international laws and policies (Guide for the Care and Use of Laboratory Animals, The National Academies Press, 8th Ed., 2011). This experimental protocol was approved by the Kangwon National University-Institutional Animal Care and Use Committee (approval no. KW-151127-1). Rats were randomly divided into (1) sham CA operated group ($n = 5$ at each time point), which received no CA operation, and (2) CA operated group, which received CA operation ($n = 9$ at each time point). We used the survived rats as follows: $n = 7$ at 6 hours, $n = 6$ at 12 hours, $n = 5$ at 1 day, and $n = 3$ at 2 days, respectively, after CA.

Induction of CA, and cardiopulmonary resuscitation (CPR)

CA induction and CPR was performed according to published

protocols (Drabek et al., 2014a, b). In short, we anesthetized the animals with 2–3% isoflurane, and mechanically ventilated them to maintain respiration using a rodent ventilator (Harvard Apparatus, Holliston, MA, USA). An oxygen saturation probe of pulse oximetry (Nonin Medical Inc, Plymouth, MN, USA) was attached to the left foot to monitor peripheral oxygen saturation (SpO_2). Body temperature (37 ± 0.5°C) was controlled during and after the CA surgery. Electrocardiographic probes (GE healthcare, Milwaukee, WI, USA) were placed in limbs for electrocardiogram (ECG), and the data were continuously monitored. The left femoral artery was cannulated under monitoring the mean arterial pressure (MAP) (MLT 1050/D, AD Instruments, Bella Vista, Austria), and the right femoral vein was cannulated for injection. We injected 2 mg of vecuronium bromide (GensiaSicor Pharmaceuticals, Irvine, CA, USA) intravenously after 5 minutes of stabilization period, stopped anesthesia, and stopped mechanical ventilation. MAP below 25 mmHg and subsequent pulseless electric activity were checked to define CA (Han et al., 2010; Che et al., 2011), which was confirmed at 3–4 minutes after vecuronium bromide injection. CPR was initiated at 5 minutes after CA by a bolus injection of sodium bicarbonate (1 meq/kg) and epinephrine (0.005 mg/kg), and followed by mechanical ventilation with 100% oxygen. Mechanical chest compression was given at a rate of 300/min until the MAP reached 60 mmHg as well as electrocardiographic activity was observed. The animals were hemodynamically stable, breathed spontaneously at 1 hour after RoSC, extubated 2 hours after resuscitation, and monitored for outcome evaluation.

Tissue preparation for histology

We anesthetized the rats with sodium pentobarbital (30 mg/kg, i.p.) and perfused them *via* the aorta with 4% paraformaldehyde. The brains were removed, embedded in tissue-freezing medium, and serially sectioned into 30 μm coronal sections using a cryostat (Leica Microsystems GmbH, Wetzlar, Germany). For tissue staining, five brain tissue sections were chosen with 120 μm interval between two sections in each animal.

Hematoxylin-eosin (HE) staining

HE staining was performed to examine acidosis and abnormal morphology. We carried out HE staining according to general protocol. Briefly, the sections were mounted on slides and stained with HE. After dehydration, the sections were mounted with Canada balsam (Kanto, Tokyo, Japan).

Cresyl violet (CV) and Fluoro-Jade B (F- J B) staining

The hippocampal sections were stained with CV according to our protocol (Park et al., 2015) to observe the rough endoplasmic reticulum (rER) in neurons in the hippocampus after CA. Shortly, we prepared 1% CV acetate (Sigma-Aldrich, St. Louis, MO, USA) in distilled water and added glacial acetic acid to the solution. We stained the hippocampal sections and mounted them with Canada balsam (Kanto, Tokyo, Japan).

We carried out F-J B histofluorescence staining to observe neuronal damage/death (degeneration) using a published method (Park et al., 2015). Briefly, we immersed the sections in 1% sodium hydroxide solution (in 80% ethanol), followed in 70% ethanol, transferred them to 0.06% potassium permanganate solution and, finally, to 0.0004% F-J B (Histochem, Jefferson, AR, USA)

Table 1 Physiologic variables in the sham-operated and CA-operated rats

	Baseline	During CA	Sham CA	6 hours post-CA	12 hours post-CA	1 day post-CA	2 days post-CA
Body weight (g)	299.8±54.0	–	289.0±80.0	297.1±93.0	297.3±57.0	296.2±92.0	294.7±51.0
Temperature (°C)	36.6±0.3	35.1±0.9		36.7±0.6	36.4±0.5	36.4±0.7	36.9±0.8
Asphyxial time to CA (second)	–	–		176.0±37.0	182.0±49.0	181.0±17.0	175.0±37.0
CPR time (minute)	–	–		1.8.0±0.7.0	1.7±0.6	1.7.0±0.9	1.6.0±0.3
MAP (mmHg)	121.0±19.0	–	117.0±23.0	111.0±24.0	115.0±27.0	113.0±31.0	114.0±54.0
Heart rate (beats/min)	347.0±18.0	–	337.0±27.0	367.0±37.0	351.0±46.0	341.0±38.0	337.0±49.0
SpO$_2$ (%)	94.0±2.6	–	97.0±13.0	80.0±8.3	67.0±6.7[*]	48.0±6.7[*]	43.0±7.4[*]

Data are expressed as the mean ± SEM (n = 9) and were analyzed using one-way analysis of variance followed by the least significant difference *post hoc* test. *P < 0.05, *vs.* baseline. CA: Cardiac arrest; CPR: cardiopulmonary resuscitation; MAP: mean arterial pressure; SpO$_2$: peripheral oxygen saturation.

solution. After staining, we examined the sections on the epi-fluorescent microscope with blue (450–490 nm) excitation light (Carl Zeiss, Göttingen, Germany). The numbers of CV and F-J B positive cells were counted according to our previously published method (Park et al., 2015). In brief, digital images of the hippocampus were captured with an AxioM1 light microscope (Carl Zeiss, Germany) equipped with a digital camera (Axiocam, Carl Zeiss, Germany) connected to a PC monitor. The cells were counted in a 250 × 250 μm square applied approximately at the center of the hippocampal CA1 region using an image analyzing system (software: Optimas 6.5, CyberMetrics, Scottsdale, AZ, USA). The studied tissue sections were selected with 120-μm interval, and cell counts were obtained by averaging the total cell numbers of 8 sections taken from each animal per group.

Immunohistochemistry
Iba-1, GFAP and TNF-α immunohistochemistry was done according to our published method (Jia et al., 2008) as follows. We incubated the sections with a rabbit anti-ionized calcium-binding adapter molecule 1 (Iba-1, 1:800, Chemicon, Temecula, CA, USA) for microglia, mouse anti-glial fibrillary acidic protein (GFAP, 1:800, Chemicon) for astrocytes and rabbit anti-TNF-α for inflammation (1:500, Abcam Incorporated, Cambridge, MA, USA), reacted it with secondary antibody, biotinylated goat anti-rabbit or horse anti-mouse IgG (1:250, Vector Laboratories Inc., Burlingame, CA, USA), developed it using Vectastain ABC (Vector Laboratories Inc.), and visualized the reacted sections in solution of 3, 3'-diaminobenzidine. For quantitative analysis of densities of GFAP, Iba-1 and TNF-α immunoreactivities, we evaluated the staining intensity of the immunoreactive structures based on an optical density (OD) obtained after transformation of the mean gray level of the immunoreactivities using a formula: OD = log (256/mean gray level). We subtracted the density of the background, and calibrated the ration of the OD of the image file using Adobe Photoshop 8.0, and we analyzed them as percent to compare them with the sham CA operated group designated as 100% using NIH Image 1.59 (version 1.46; NIH Image, Bethesda, MD, USA).

Statistical analysis
All data were entered into SAS (version 9.02; SAS Institute Inc., Cary, NC, USA) and presented as the mean ± SEM. Survival rate was analyzed using Kaplan-Meier survival analysis and log-rank test. Statistical analyses of physiologic variables and semi-quantitative analysis for histopathology and immunoreactivities of
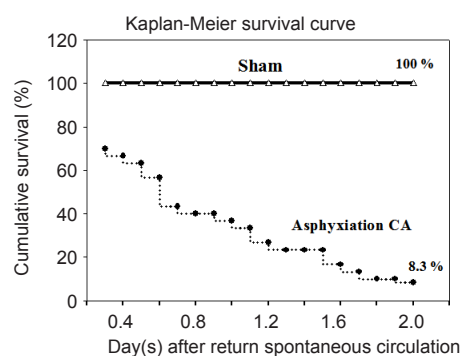

Figure 1 Cumulative survival rate using Kaplan-Meier analysis in the sham- (unbroken line) and CA (broken line)-operated groups for 2 days after return of spontaneous circulation (ROSC).
The CA-operated group had significantly different survival rate from the sham-operated group (log-rank test, P < 0.05). CA: Cardiac arrest.

Iba-1, GFAP and TNF-α were conducted using one-way analysis of variance (ANOVA). To determine the significance of differences, the least significant difference *post hoc* test was conducted for all pairwise multiple comparisons. Differences were considered significant when P value was less than 0.05.

Results
Physiological variables
There were no significant differences in baseline characteristics between the sham-operated and CA-operated groups (P > 0.05) (**Table 1**). Body weight was not altered in the CA-operated group. Body temperature and heart rate were the same as those at the baseline or after ROSC. CA was confirmed by isoeletric electrocardiogram (ECG), mean arterial pressure (MAP) and SpO$_2$. In the CA-operated group, MAP and SpO$_2$ were altered as expected.

Survival rate
The survival rate in the CA-operated group was 100% at 6 hours post-CA, and the survival rate was reduced with time post-CA, showing about 63.3% at 12 hours, 36.7% at 1 day and 8.3 % at 2 days post-CA (**Figure 1**).

HE staining results
HE staining was performed to detect acidosis of inflammatory response and abnormal morphology in the hippocampus after CA (**Figure 2**). In the sham CA-operated rats, cells of the stratum pyramidale in the hippocampal subregions (CA1-3 regions)
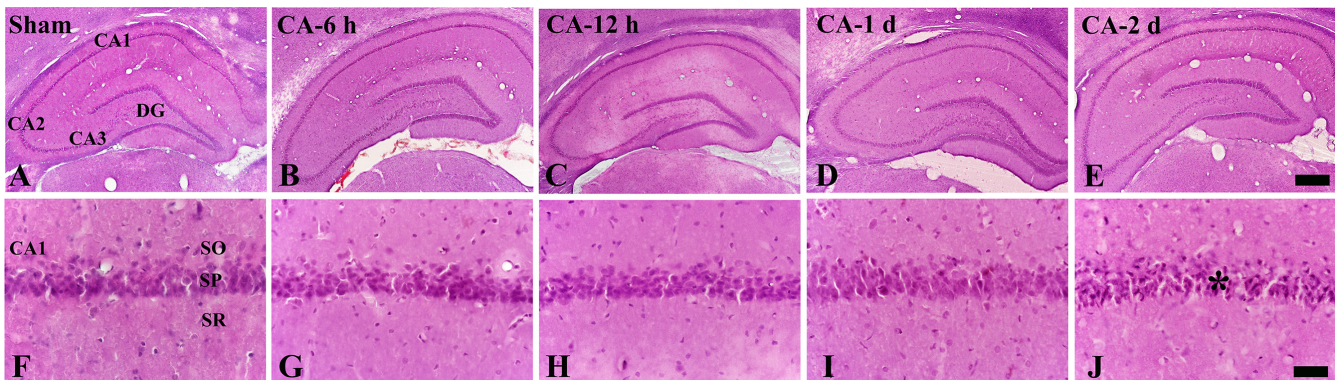
Figure 2 Hematoxylin-eosin (HE) staining of the hippocampus of the sham and cardiac arrest (CA) operated rats.
(A–E) Low magnification of the hippocampus. (F–J) High magnification of the CA1 region. Histopathological change is not found in the CA-operated rats until 1 day (d) post-CA. At 2 d post-CA, cells of the stratum pyramidale (SP, asterisk) of the CA1 region, not the other sub-regions, are shrunk. CA1–3: Cornu ammonis 1–3; DG: dentate gyrus; SO: stratum oriens; SR: stratum radiatum. Scale bars: 200 μm (A–E) and 50 μm (F–J). h: Hours.
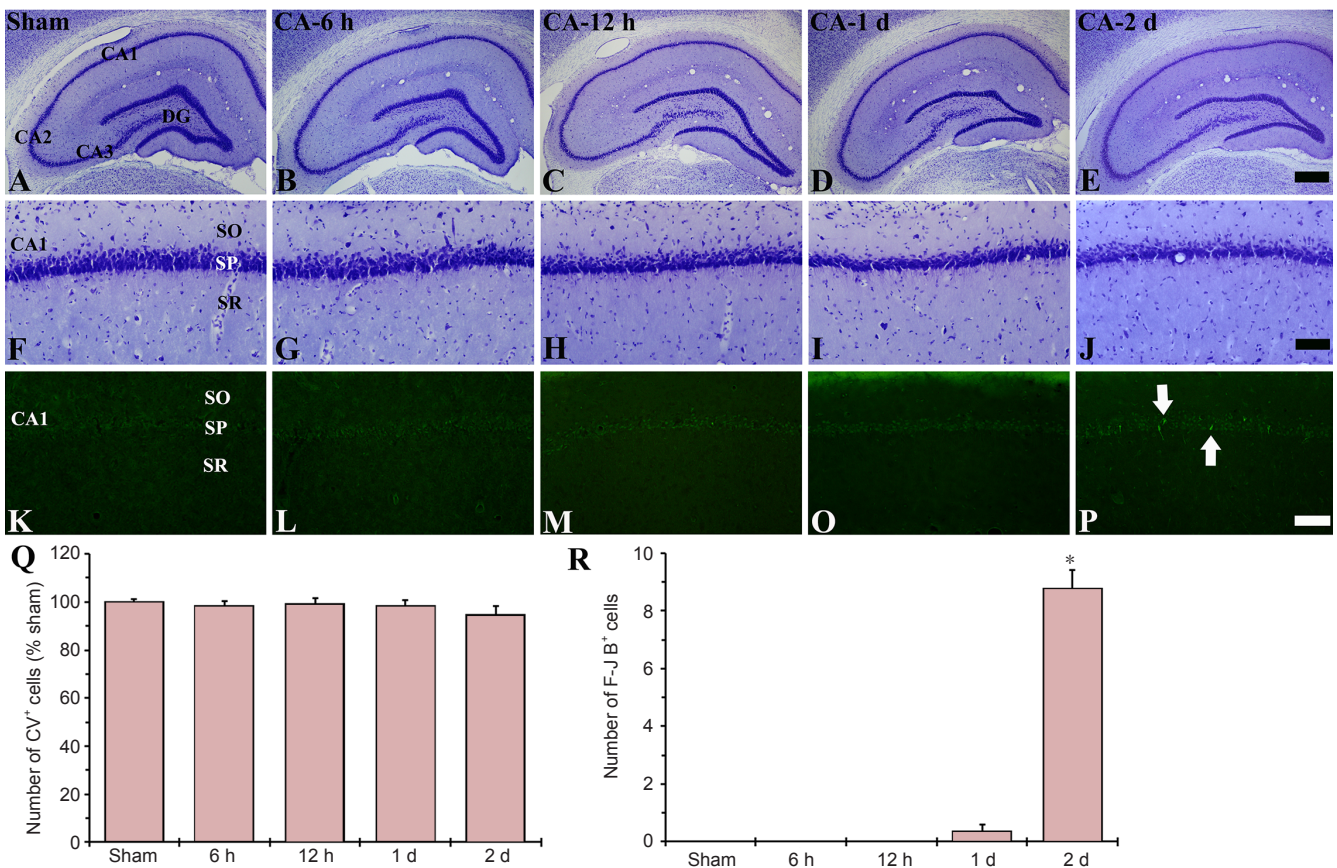

Figure 3 CV (A-J) and F-J B (K-P) staining of the hippocampus of the sham and cardiac arrest (CA) operated rats.
(A–P) CV (A–J) and F-J B (K–P) staining in the hippocampus of rats. CV staining in all CA-operated rats is not significantly different from that in the sham CA operated rats. Some F-J B-positive cells (green, white arrows) are detected in the stratum pyramidale (SP) of the CA1 region alone at 2 days post-CA. Scale bars: 200 μm (A–E) and 50 μm (F–P). Relative analysis as percentage in mean numbers of CV- (Q) and F-J B-positive cells (R) (n = 7 at 6 h, n = 6 at 12 h, n = 5 at 1 d, and n = 3 at 2 d post-CA; *P < 0.05, *vs.* sham-operated (sham) group; one-way analysis of variance followed by the least significant difference *post hoc* test). The bars indicate the mean ± SEM. CV: Cresyl violet; F-J B: Fluoro-Jade B; CA1–3: Cornu ammonis 1–3; DG: dentate gyrus; SO: stratum oriens; SR: stratum radiatum; h: hours; d: day(s).

and cells of the granule cell layer of the dentate gyrus were easily detected (**Figure 2A, F**). In the CA-operated rats, no significant change was found in the hippocampus until 1 day post-CA, although acidosis was shown in cells of the stratum pyramidale of the CA1 area (**Figure 2B–D, G–I**). However, 2 days post-CA, cells in the stratum pyramidale were markedly shrunk in the

CA1 region, but not in the other subregions (**Figure 2J**).

CV staining results
rER change in neurons was examined in the hippocampus using CV staining (**Figure 3A–J**). Cells of the stratum pyramidale in the CA1-3 regions and cells of the granule cell layer in the
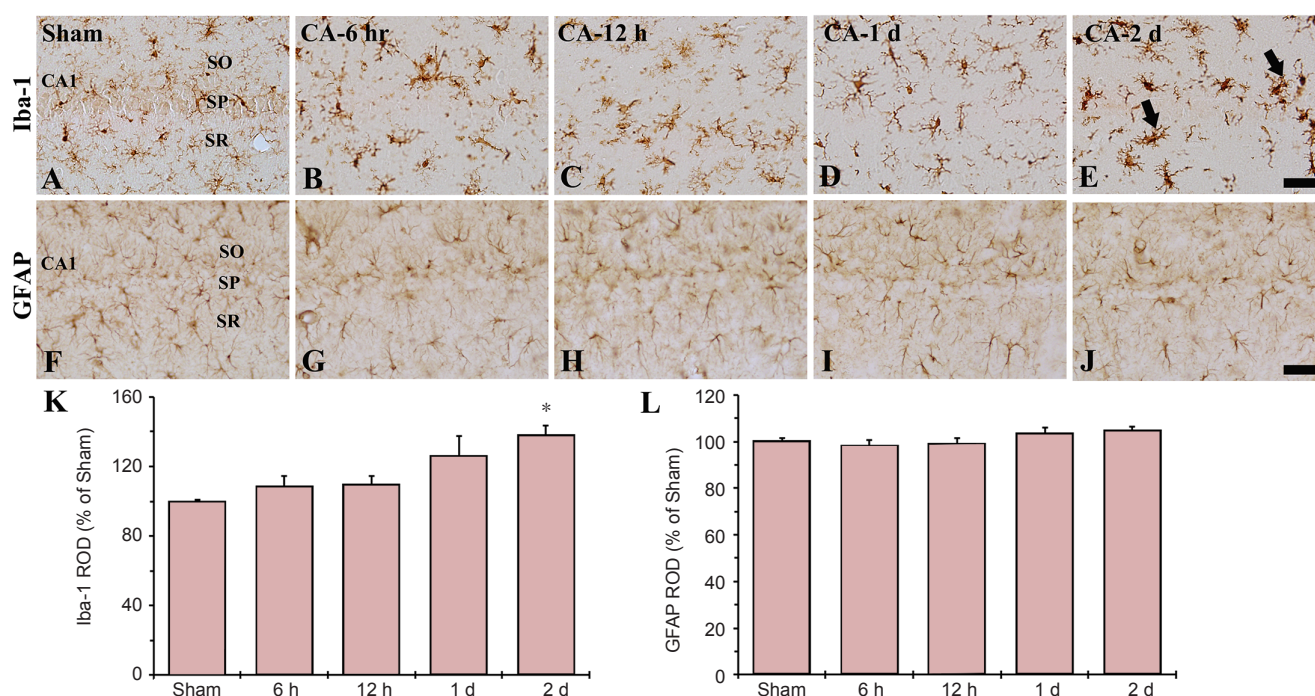
Figure 4 Iba-1 and GFAP immunoreactivity in the CA1 region of the hippocampus in the sham and cardiac arrest (CA) operated rats.
(A–J) Immunohistochemical staining for Iba-1 (A–E) and GFAP (F–J). Iba-1-immunoreactive microglia (arrows) in the CA operated rats are enlarged in all layers of the CA1 region at 2 days (d) post-CA. GFAP-immunoreactive astrocytes in the CA operated rats are not altered until 2 d post-CA. Scale bars: 50 μm. Relative optical density (ROD) as percentage values of the Iba-1 (K) and GFAP (L) immunoreactivity ($n = 7$ at 6 hours (h), $n = 6$ at 12 h, $n = 5$ at 1 d, and $n = 3$ at 2 d after CA; $*P < 0.05$, *vs.* sham-operated (sham) group; one-way analysis of variance followed by the least significant difference *post hoc* test). The bars indicate the mean ± SEM. CA1: Cornu ammonis 1; SO: stratum oriens; SP: stratum pyramidale; SR: stratum radiatum; Iba-1: ionized calcium-binding adapter molecule 1; GFAP: glial fibrillary acidic protein; h(r): hours; d: day(s).
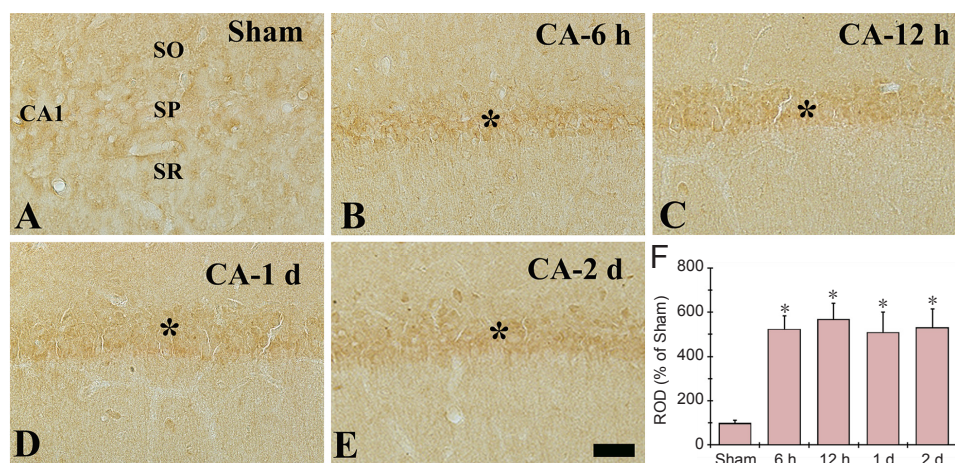

(A–E) Relative to the sham group (A), TNF-α immunoreactivity (asterisk) increased in cells of the stratum pyramidale at 6 hours post-CA (B), and maintained until 2 d post-CA (C–E asterisk). Scale bar: 50 μm. (F) Relative optical density (ROD) of TNF-α-immunoreactive cells ($n = 7$ at 6 h, $n = 6$ at 12 h, $n = 5$ at 1 d, and $n = 3$ at 2 d post-CA; $*P < 0.05$, *vs.* sham operated (sham) group; one-way analysis of variance followed by the least significant difference *post hoc* test). The bars indicate the mean ± SEM. CA1: Cornu ammonis 1; SO: stratum oriens; SP: stratum pyramidale; SR: stratum radiatum; ROD: relative optical density.

Figure 5 Immunohistochemistry for tumor necrosis factor-alpha (TNF-α) in the CA1 region of the hippocampus in the sham and cardiac arrest (CA) operated rats.

dentate gyrus were well stained with CV in the sham CA-operated rats (**Figure 3A, F**). In the CA-operated groups, significant change was not found in the CV-positive cells compared with those in the sham CA-operated rats (**Figure 3B–E, G–I, and Q**).

F-J B staining results
F-J B-positive cells, which are dead cells, were not found in any regions of the sham CA operated rats (Figure 3K). In the CA operated rats, F-J B-positive cells were not detected in any region until 1 day post-CA (**Figure 3L–O**); however, 2 days

post-CA, some F-J B-positive cells were shown in the stratum pyramidale of the CA1 region, but not in the other sub-regions (**Figure 3P, R**).

Iba-1 immunoreactivity
In the sham CA operated rats, Iba-1-immunoreactive microglia were scattered in all layers in the CA1 region, showing that they were ramified as resting form (**Figure 4A**). In the CA operated rats, Iba-1-immunoreactive microglia was not activated at 1 day after CA (**Figure 4B–D**). However, at 2 days post-CA, Iba-1-im-

munoreactive microglia were activated, namely, they had enlarged cell bodies with short and thicken processes (**Figure 4E, K**).

GFAP immunoreactivity

In the sham CA operated rats, GFAP-immunoreactive cells as astrocytes showed resting form, which had small cell bodies with thread like thin processes, and they were distributed in all layers in the CA1 region (**Figure 4F**). In the CA operated rats, GFAP-immunoreactive astrocytes were not changed in all groups (**Figure 4G–J, L**).

TNF-α immunohistochemistry

We examined inflammatory response in the CA1 region after CA using TNF-α immunohistochemistry (**Figure 5**). TNF-α immunoreactivity was weak in the sham CA operated rats (**Figure 5A**). In the CA operated rats, TNF-α immunoreactivity was significantly increased in the cells of the stratum pyramidale at 6 hours post-CA (**Figure 5B, F**), thereafter, TNF-α immunoreactivity in the cells maintained until 2 days post-CA (**Figure 5C–F**).

Discussion

PCAS is the main cause of mortality in the early stage after CA (Roberts et al., 2013; Cour et al., 2014). The survival rate of out-of-hospital CA patients who were administered CPR by ambulance staff, was reported to be 14.6%. Only 39% of them survived during admission, and half of them died within the first 24 hours in the hospital (Cobbe et al., 1996; Berdowski et al., 2010; Roberts et al., 2013). Che et al. (2011) reported that survival rate was about 40% at 2 days after RoSC in a rat model of asphyxial CA. In contrast, Kida et al. (2014) reported that all mice died within 1 day after RoSC in a mouse model of potassium induced CA. In our present study, the survival rate decreased immediately after RoSC and reached about 5% 2 days after RoSC. Experimental animals die within at least 2 days after CA, although, as described above, the survival rate in animal models of CA is different according to methods or animals used. In this regard, we conducted histopathological evaluations in the rat hippocampus that is most vulnerable to ischemia/reperfusion injury in the early stage after CA.

In the present study, significant neuronal death in the CA-induced rat hippocampus was not shown until 1 day post-CA under normothermia; however, some neurons died in the stratum pyramidale of the hippocampal CA1 area 2 days post-CA, although the survival rate at that time was about 5%. To our best knowledge, no studies regarding neuronal death in the hippocampus during the early stage after CA have been reported. Instead, many researchers have reported that neurons of the stratum pyramidale in the CA1 region of the hippocampus die at least 4 or 5 days after transient global cerebral ischemia in rodents (Treasure et al., 1983; Drabek et al., 2014a; Li et al., 2015). Our present data, compared to results using transient cerebral ischemia, suggest that early death of CA-induced animal models must be caused by other factors, not neuronal loss in the brain.

Astrocytes perform many functions, including biochemical support of the blood-brain barrier, maintenance of extracellular ion balance, supply of nutrients to the nervous tissue, and roles in repair and scarring process of the CNS following injuries (Park et al., 2015). Meanwhile, microglia are key glial cells in overall brain maintenance, namely, they are constantly scaveng-

ing the central nervous system for damaged or unnecessary neurons, and infectious agents following injuries (Park et al., 2014). Thus, activation of astrocyte and microglia (gliosis) was important for pathological response in the brain. Many studies have been carried out regarding gliosis (microgliosis and astrocytosis) in the CA1 region of the hippocampus after transient global cerebral ischemia in rodents (Roberts et al., 2013; Drabek et al., 2014b; Park et al., 2014, 2015). They reported that microglial cells were activated in the hippocampal CA1 region from about 2 days post-ischemia and many of the activated microglia were aggregated near the stratum pyramidale from several days (4 or 5 days) after transient ischemia. The researchers, in addition, reported that astrocytes were significantly activated throughout all layers of the ischemic CA1 area several days after transient ischemia. In this study, Iba-1-immunoreactive microglia in the CA1 region did not change until 1 day post-CA, and they were activated (enlarged cell bodies with short and thicken processes) in all layers 2 days post-CA. On the contrary, GFAP-immunoreactive astrocytes did not change significantly until 2 days post-CA. Compared to the findings in transient global cerebral ischemia, our present study indicates that gliosis in the CA1 area following CA is not significant, although microglia are activated throughout all layers 2 days post-CA. This finding suggests that animals die before developing active gliosis as well as neuronal loss (death) after CA under normothermia.

The pathophysiology of PCAS is complex and partially understood (Mongardon et al., 2011). CA-induced injuries, including inflammatory response, are caused by a systemic response to global ischemia/reperfusion insult, (Neumar et al., 2008; Roberts et al., 2013), and the pattern of CA-induced inflammatory response is comparable to that observed in septic shock (Adrie et al., 2002; Neumar et al., 2008). Inflammatory response after RoSC is characterized by ROS production, adhesion molecule expression, polymorphonuclear leukocyte activation, and release of cytokines such as TNF-α (Bro-Jeppesen et al., 2014). However, their mechanisms in PCAS are still unclear. Inflammatory cytokines have been suggested to play important roles in the pathophysiology of PCAS and they are implicated in myocardial and brain dysfunction in the early stage after CA (Youngquist et al., 2009, 2013). Adrie et al. (2002) reported that pro-inflammatory cytokines increased following resuscitation. In particular, Zhao et al. (2015) recently reported that TNF-α increases shortly after RoSC, which was predictive of early death, and suggested that the plasma level of TNF-α was inversely correlated with myocardial function after CA. TNF-α, a pro-inflammatory cytokine and a master regulator of inflammatory response, is primarily produced by macrophages and by a broad variety of cell types including mast-cells, lymphoid cells, endothelial cells, myocytes, adipose cells, and neurons following CA (Youngquist et al., 2013). Recently, TNF-α protein levels were reported to increase in the left ventricle of the heart after 6 hours post-CA (Drabek et al., 2014b; Zhao et al., 2015). In addition, Qi et al. (2013) reported a significant increase in TNF-α protein level in the lung of an animal model of cardiopulmonary bypass. In the present study, we found that TNF-α immunoreactivity increased significantly in the hippocampal CA1 region from 6 hours after CA. Based on the above-mentioned reports, we suggest that an early increase in the TNF-α immunoreactivity in the hippocampus after CA is

related to early death after CA in animal models of CA.

In brief, most rats died within 2 days after CA, showing that some neurons died and moderate microgliosis, not astrocytosis, appeared in the hippocampus 2 days after CA. In addition, TNF-α immunoreactivity increased significantly in the hippocampus in the early stage after CA. In this regard, it needs to investigate whether TNF-α is related with the death of rats before 2 days after CA.

References

Adrie C, Adib-Conquy M, Laurent I, Monchi M, Vinsonneau C, Fitting C, Fraisse F, Dinh-Xuan AT, Carli P, Spaulding C, Dhainaut JF, Cavaillon JM (2002) Successful cardiopulmonary resuscitation after cardiac arrest as a "sepsis-like" syndrome. Circulation 106:562-568.

Berdowski J, Berg RA, Tijssen JG, Koster RW (2010) Global incidences of out-of-hospital cardiac arrest and survival rates: Systematic review of 67 prospective studies. Resuscitation 81:1479-1487.

Bro-Jeppesen J, Kjaergaard J, Wanscher M, Nielsen N, Friberg H, Bjerre M, Hassager C (2014) The inflammatory response after out-of-hospital cardiac arrest is not modified by targeted temperature management at 33 degrees C or 36 degrees C. Resuscitation 85:1480-1487.

Bro-Jeppesen J, Kjaergaard J, Wanscher M, Nielsen N, Friberg H, Bjerre M, Hassager C (2015) Systemic inflammatory response and potential prognostic implications after out-of-hospital cardiac arrest: a substudy of the target temperature management trial. Crit Care Med 43:1223-1232.

Che D, Li L, Kopil CM, Liu Z, Guo W, Neumar RW (2011) Impact of therapeutic hypothermia onset and duration on survival, neurologic function, and neurodegeneration after cardiac arrest. Crit Care Med 39:1423-1430.

Cobbe SM, Dalziel K, Ford I, Marsden AK (1996) Survival of 1476 patients initially resuscitated from out of hospital cardiac arrest. BMJ 312:1633-1637.

Cour M, Abrial M, Jahandiez V, Loufouat J, Belaidi E, Gharib A, Varennes A, Monneret G, Thibault H, Ovize M, Argaud L (2014) Ubiquitous protective effects of cyclosporine A in preventing cardiac arrest-induced multiple organ failure. J Appl Physiol (1985) 117:930-936.

Drabek T, Foley LM, Janata A, Stezoski J, Kevin Hitchens T, Manole MD, Kochanek PM (2014a) Global and regional differences in cerebral blood flow after asphyxial versus ventricular fibrillation cardiac arrest in rats using ASL-MRI. Resuscitation 85:964-971.

Drabek T, Janata A, Wilson CD, Stezoski J, Janesko-Feldman K, Tisherman SA, Foley LM, Verrier JD, Kochanek PM (2014b) Minocycline attenuates brain tissue levels of TNF-alpha produced by neurons after prolonged hypothermic cardiac arrest in rats. Resuscitation 85:284-291.

Girotra S, Chan PS, Bradley SM (2015) Post-resuscitation care following out-of-hospital and in-hospital cardiac arrest. Heart 101:1943-1949.

Han F, Boller M, Guo W, Merchant RM, Lampe JW, Smith TM, Becker LB (2010) A rodent model of emergency cardiopulmonary bypass resuscitation with different temperatures after asphyxial cardiac arrest. Resuscitation 81:93-99.

Jia X, Koenig MA, Shin HC, Zhen G, Pardo CA, Hanley DF, Thakor NV, Geocadin RG (2008) Improving neurological outcomes post-cardiac arrest in a rat model: immediate hypothermia and quantitative EEG monitoring. Resuscitation 76:431-442.

Kida K, Shirozu K, Yu B, Mandeville JB, Bloch KD, Ichinose F (2014) Beneficial effects of nitric oxide on outcomes after cardiac arrest and cardiopulmonary resuscitation in hypothermia-treated mice. Anesthesiology 120:880-889.

Laubach VE, Sharma AK (2016) Mechanisms of lung ischemia-reperfusion injury. Curr Opin Organ Transplant 21:246-252.

Laurent I, Monchi M, Chiche JD, Joly LM, Spaulding C, Bourgeois B, Cariou A, Rozenberg A, Carli P, Weber S, Dhainaut JF (2002) Reversible myocardial dysfunction in survivors of out-of-hospital cardiac arrest. J Am Coll Cardiol 40:2110-2116.

Li J, Wang H, Zhong Q, Zhu X, Chen SJ, Qian Y, Costakis J, Bunney G, Beiser DG, Leff AR, Lewandowski ED, JM OD, Vanden Hoek TL (2015) A novel pharmacological strategy by PTEN inhibition for improving metabolic resuscitation and survival after mouse cardiac arrest. Am J Physiol Heart Circ Physiol 308:H1414-1422.

Lopez-Herce J, del Castillo J, Matamoros M, Canadas S, Rodriguez-Calvo A, Cecchetti C, Rodriguez-Nunez A, Carrillo A (2014) Post return of spontaneous circulation factors associated with mortality in pediatric in-hospital cardiac arrest: a prospective multicenter multinational observational study. Crit Care 18:607.

Madl C, Holzer M (2004) Brain function after resuscitation from cardiac arrest. Curr Opin Crit Care 10:213-217.

Mongardon N, Dumas F, Ricome S, Grimaldi D, Hissem T, Pene F, Cariou A (2011) Postcardiac arrest syndrome: from immediate resuscitation to long-term outcome. Ann Intensive Care 1:45.

Neumar RW, Nolan JP, Adrie C, Aibiki M, Berg RA, Böttiger BW, Callaway C, Clark RS, Geocadin RG, Jauch EC, Kern KB, Laurent I, Longstreth WT Jr, Merchant RM, Morley P, Morrison LJ, Nadkarni V, Peberdy MA, Rivers EP, Rodriguez-Nunez A, et al. (2008) Post-cardiac arrest syndrome: epidemiology, pathophysiology, treatment, and prognostication. A consensus statement from the International Liaison Committee on Resuscitation (American Heart Association, Australian and New Zealand Council on Resuscitation, European Resuscitation Council, Heart and Stroke Foundation of Canada, InterAmerican Heart Foundation, Resuscitation Council of Asia, and the Resuscitation Council of Southern Africa); the American Heart Association Emergency Cardiovascular Care Committee; the Council on Cardiovascular Surgery and Anesthesia; the Council on Cardiopulmonary, Perioperative, and Critical Care; the Council on Clinical Cardiology; and the Stroke Council. Circulation 118:2452-2483.

Park JH, Shin BN, Chen BH, Kim IH, Ahn JH, Cho JH, Tae HJ, Lee JC, Lee CH, Kim YM, Lee YL, Kim SK, Won MH (2015) Neuroprotection and reduced gliosis by atomoxetine pretreatment in a gerbil model of transient cerebral ischemia. J Neurol Sci 359:373-380.

Park JH, Park O, Cho JH, Chen BH, Kim IH, Ahn JH, Lee JC, Yan BC, Yoo KY, Lee CH, Hwang IK, Kwon SH, Lee YL, Won MH, Choi JH (2014) Anti-inflammatory effect of tanshinone I in neuroprotection against cerebral ischemia-reperfusion injury in the gerbil hippocampus. Neurochem Res 39:1300-1312.

Qi D, Gao MX, Yu Y (2013) Intratracheal antitumor necrosis factor-alpha antibody attenuates lung tissue damage following cardiopulmonary bypass. Artif Organs 37:142-149.

Roberts BW, Kilgannon JH, Chansky ME, Mittal N, Wooden J, Parrillo JE, Trzeciak S (2013) Multiple organ dysfunction after return of spontaneous circulation in postcardiac arrest syndrome. Crit Care Med 41:1492-1501.

Treasure T, Naftel DC, Conger KA, Garcia JH, Kirklin JW, Blackstone EH (1983) The effect of hypothermic circulatory arrest time on cerebral function, morphology, and biochemistry. An experimental study. J Thorac Cardiovasc Surg 86:761-770.

Youngquist ST, Niemann JT, Heyming TW, Rosborough JP (2009) The central nervous system cytokine response to global ischemia following resuscitation from ventricular fibrillation in a porcine model. Resuscitation 80:249-252.

Youngquist ST, Niemann JT, Shah AP, Thomas JL, Rosborough JP (2013) A comparison of etanercept vs. infliximab for the treatment of post-arrest myocardial dysfunction in a swine model of ventricular fibrillation. Resuscitation 84:999-1003.

Zhao ZG, Tang ZZ, Zhang WK, Li JG (2015) Protective effects of embelin on myocardial ischemia-reperfusion injury following cardiac arrest in a rabbit model. Inflammation 38:527-533.

Copyedited by Li CH, Song LP, Zhao M